Abdominal Radiology (2019) 44:3935–3949
https://doi.org/10.1007/s00261-019-02127-8

SPECIAL SECTION: UROTHELIAL DISEASE

Multimodality imaging of the male urethra: trauma, infection, neoplasm, and common surgical repairs

David D. Childs[1] · Ray B. Dyer[1] · Brenda Holbert[1] · Ryan Terlecki[2] · Jyoti Dee Chouhan[2] · Jao Ou[1]

Published online: 22 August 2019

Abstract

Objective The aim of this article is to describe the indications and proper technique for RUG and MRI, their respective image findings in various disease states, and the common surgical techniques and imaging strategies employed for stricture correction.

Results Because of its length and passage through numerous anatomic structures, the adult male urethra can undergo a wide array of acquired maladies, including traumatic injury, infection, and neoplasm. For the urologist, imaging plays a crucial role in the diagnosis of these conditions, as well as complications such as stricture and fistula formation. While retrograde urethrography (RUG) and voiding cystourethrography (VCUG) have traditionally been the cornerstone of urethral imaging, MRI has become a useful adjunct particularly for the staging of suspected urethral neoplasm, visualization of complex posterior urethral fistulas, and problem solving for indeterminate findings at RUG.

Conclusions Familiarity with common urethral pathology, as well as its appearance on conventional urethrography and MRI, is crucial for the radiologist in order to guide the treating urologist in patient management.

Keywords Urethra · Retrograde urethrography · Magnetic resonance imaging · Stricture

Introduction

Medical imaging plays a crucial role in the diagnosis, treatment planning, and follow-up of a wide variety of male urethral diseases. Some of the most common indications for urethral imaging include suspected traumatic injury, stricture disease, neoplasm, and fistula development. Traditionally, the cornerstone of male urethral imaging has been retrograde urethrography (RUG) and voiding cystourethrography (VCUG), during which intraluminal contrast media allows visualization of the anterior and posterior urethra, respectively. While the urethral mucosa is well depicted with these radiographic examinations, the periurethral soft tissues are not. More recently, MRI has become increasingly recognized as a powerful tool for this task. An understanding of abnormalities visible on any of these diagnostic examinations, however, requires a thorough knowledge of male reproductive anatomy.

In this study, we will review male urethral anatomy as depicted on urethrography and MRI. We additionally describe the proper technique for RUG, VCUG, and MRI, as well as their use in the diagnosis and treatment planning of traumatic urethral injury, stricture disease, neoplasm, and fistula. Finally, we discuss the common techniques of urethroplasty for the surgical correction of anterior urethral strictures, as well as the role of imaging.

CME activity This article has been selected as the CME activity for the current month. Please visit https://ce.mayo.edu/node/87862 and follow the instructions to complete this CME activity.

✉ David D. Childs
dchilds@wakehealth.edu

[1] Department of Radiology, Wake Forest University School of Medicine, Medical Center Boulevard, Winston-Salem, NC 27157, USA

[2] Department of Urology, Wake Forest University School of Medicine, Medical Center Boulevard, Winston-Salem, NC 27157, USA

Male urethral anatomy

The male urethra is a muscular tube that extends from the bladder base to the external urethral meatus, achieving an average length of 18–20 cm (Fig. 1). By convention, it is usually divided into (1) the posterior division from

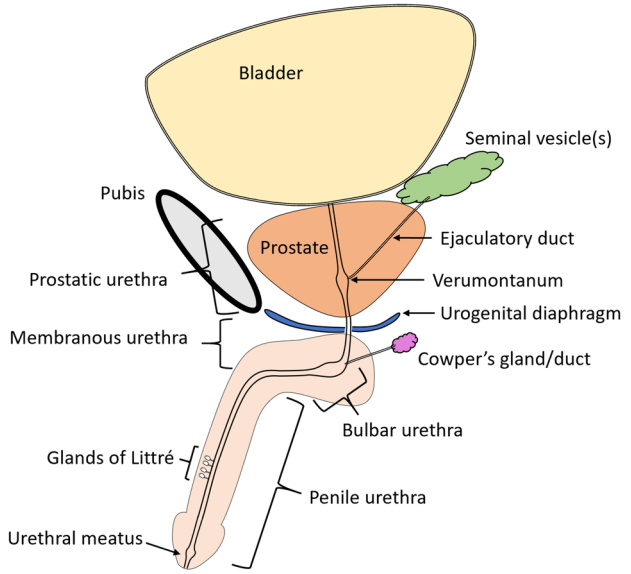

Fig. 1 Anatomy of the male urethra

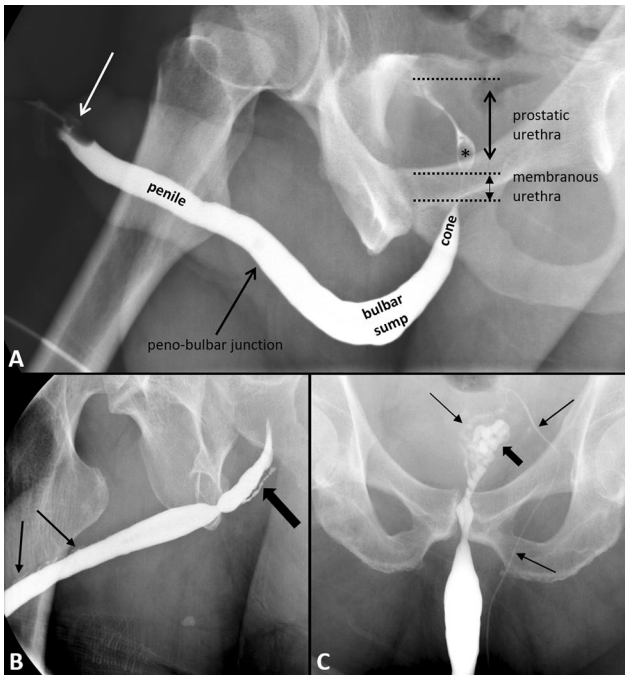

Fig. 2 **a** The urethral segments as depicted on retrograde urethrogram. Note catheter in the meatal portion (white arrow). The verumontanum is seen as an oblong filling defect (asterisk). **b** The tiny periurethral glands of Littré can sometimes be opacified (thin arrows) along the dorsal penile urethra. The Cowper ducts (thick arrow) may also opacify. **c** In rare instances, there may be opacification of the seminal vesicle (thick arrow) and even vas deferens (thin arrows)

the bladder neck to the inferior urogenital diaphragm, and (2) the anterior division from the inferior urogenital diaphragm to the external meatus at the tip of the glans penis. The posterior urethra is further divided into the prostatic (4 cm) and membranous (1–1.5 cm) segments. A longitudinal ridge of smooth muscle (urethral crest) runs along the posterior margin of the prostatic segment, and contains the verumontanum, a 1-cm ovoid mound with a central depression, the prostatic utricle. The orifices of the ejaculatory ducts empty on either side of the verumontanum, which is also flanked by multiple tiny openings of small prostatic ducts. The membranous urethra, the shortest and least distensible segment, is surrounded by the external urethral sphincter of the urogenital diaphragm and paired Cowper glands. The distal end of the verumontanum marks the proximal boundary of the membranous urethra. Lymphatic drainage of the posterior urethra is via the iliac nodes.

The anterior urethra is also further divided into two segments, the bulbous segment proximally and the penile segment distally. The bulbous segment extends from the inferior margin of the urogenital diaphragm to the penoscrotal junction and is surrounded by the corpus spongiosum. The proximal dilated portion of the bulbous urethra, the widest portion of the urethra, is commonly called the "sump," and the more superior conical shape portion at the bulbomembranous junction is commonly called the "cone," both well depicted with RUG (Fig. 2). The paired Cowper gland ducts empty into the bulbous sump segment. The penile urethra, which is of uniform caliber, extends from the penoscrotal junction to the external meatus. Numerous small periurethral (Littré) glands, along with their small draining ducts, are found predominantly along the dorsal aspect of the penile urethra. The mildly widened distal 1–1.5 cm of the penile urethra is referred to as the fossa navicularis. Lymphatic drainage of the anterior urethra is via the inguinal lymph nodes.

Urethral imaging techniques

Retrograde urethrography

RUG allows the depiction of anterior urethral luminal abnormalities [1]. The most common indications for RUG are suspected traumatic injury, stricture disease, and fistula [2]. A quality examination requires attention to technical detail. The patient should be positioned in a 45° posterior oblique orientation, followed by sterile preparation of the external genitalia. To achieve hydrostatic distention of a contrast-filled urethra, two techniques can be considered. In the more widely used balloon occlusion technique, a 5-mL balloon-tipped 14-French catheter is inserted until the balloon rests in the fossa navicularis, with subsequent inflation with 1–3 mL of fluid (Fig. 3). Lubrication or anesthetic gel can make urethral occlusion

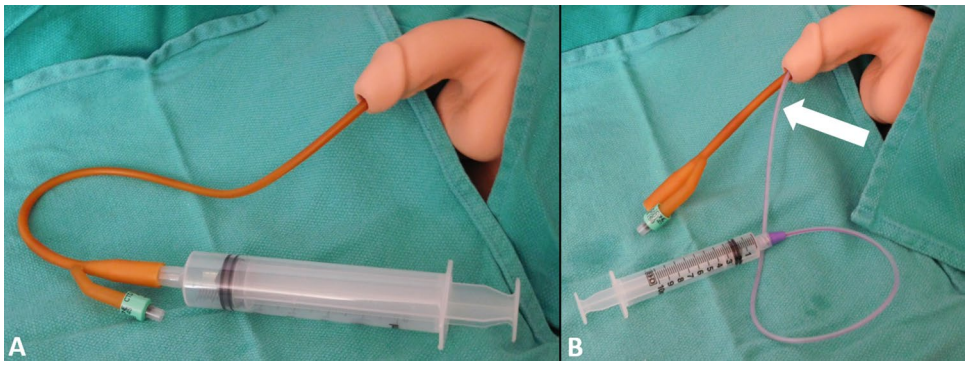

Fig. 3 Mock simulation with mannequin. A 14-Fr balloon-tipped catheter has been inserted into the meatal portion of the urethra for the RUG (**a**) and the balloon inflated with 1.5 mL of contrast media. For the pericatheter technique (**b**), a 5-Fr pediatric feeding tube (arrow) is placed alongside an existing 14-Fr catheter, below the site of surgical repair or traumatic injury

more difficult but may be required for cases of meatal stenosis [3]. Along with the application of traction to elongate the penis, 10–25 mL of iodinated contrast media is gently injected with fluoroscopic monitoring and appropriate spot imaging. In the clamp technique, a 6-French to 10-French catheter is placed and subsequently secured by a compression clamp device surrounding the glans penis, followed by contrast infusion via a gravity drip system [4]. Spasm of the external urethral sphincter is commonly encountered, preventing opacification of the deep bulbar and more proximal segments [5]. Continuous gentle pressure is then required for passage of contrast through the posterior urethra into the bladder. Occasionally, patient intolerance may preclude posterior urethral filling, making it difficult to distinguish between spasm and obliterative bulbar stricture. Release fluoroscopic images can also be obtained as the contrast media is expelled, particularly useful in cases of meatal stenosis.

In situations requiring urethral evaluation with a preexisting Foley catheter, a pericatheter RUG is indicated. After sterile preparation of the genitalia and external tubing, a small bore (5-French to 8-French) catheter is lubricated and inserted beside the existing catheter (Fig. 3). The penis can be optimally positioned by manipulation of the Foley catheter. As external pressure is applied to the glans penis, contrast media is gently injected with fluoroscopic monitoring. The catheter can be advanced more proximally as needed for improved urethral opacification.

Voiding cystourethrography

VCUG is the favored method for evaluation of the posterior urethra. This technique requires bladder filling with 350–400 mL of contrast media, as tolerated by the patient, which can be achieved by suprapubic catheter, Foley catheter, or during RUG as part of a comprehensive urethral examination [3]. The proper filling technique is dictated by the clinical scenario. During active voiding, videofluoroscopy and spot radiographs of the bladder and urethra are obtained. The bladder neck opens to a funnel shape, the

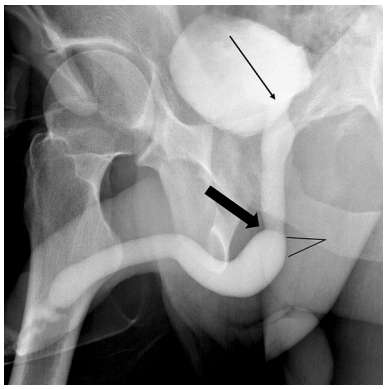

Fig. 4 During voiding, the bladder neck (thin black arrow) opens with distention of the prostatic urethra as compared to RUG. Persistent relative narrowing of the membranous urethra (thick black arrow) is normal, as it is the least distensible segment. Note the less conical shape of the proximal bulbous urethra (fanned lines)

verumontanum becomes elongated, and the proximal bulbous urethra is less conical in appearance (Fig. 4). Most patients find it easier to void in a standing or semi-upright (45°) position, although a supine position may be required if the patient is unable to stand, such as in the setting of trauma. A pericatheter technique can be used in postsurgical patients with Foley catheters present, in which the patient voids around the catheter. If no leaks are detected, a traditional VCUG can then be attempted following catheter removal.

Magnetic resonance imaging

Although much less commonly performed than conventional urethrography, MRI is a useful adjunct for evaluation of the periurethral soft tissues [6]. Patient positioning is supine with the penis at midline either resting on the anterior abdominal wall or dependently [7]. The cornerstone of penile/urethral MRI is a high-resolution, small field-of-view, thin-slice T2-weighted fast spin echo (FSE) imaging in three planes using a phased-array multichannel surface

coil, which allows the best depiction of anatomic structures. T1-weighted FSE and fat-suppressed T2-weighted imaging are useful for depiction of hematoma/corporal thrombosis and inflammation, respectively. Dynamic contrast-enhanced imaging with 3D T1 gradient echo imaging can be useful for the assessment of the cavernosal vessels and corporal enhancement but has not been shown useful for tumor staging [6, 8]. The prostatic urethra is well depicted on axial imaging as a slit-like structure that is mildly hyperintense on T2WI in comparison to the transition zone. The membranous urethra is highlighted on sagittal images as a tubular T2 hyperintense structure traversing the lower signal urogenital diaphragm (Fig. 5). The anterior urethra is seen as a lower signal structure surrounded by the high signal of the corpus spongiosum, which itself is enveloped by the low signal tunica albuginea (Fig. 5).

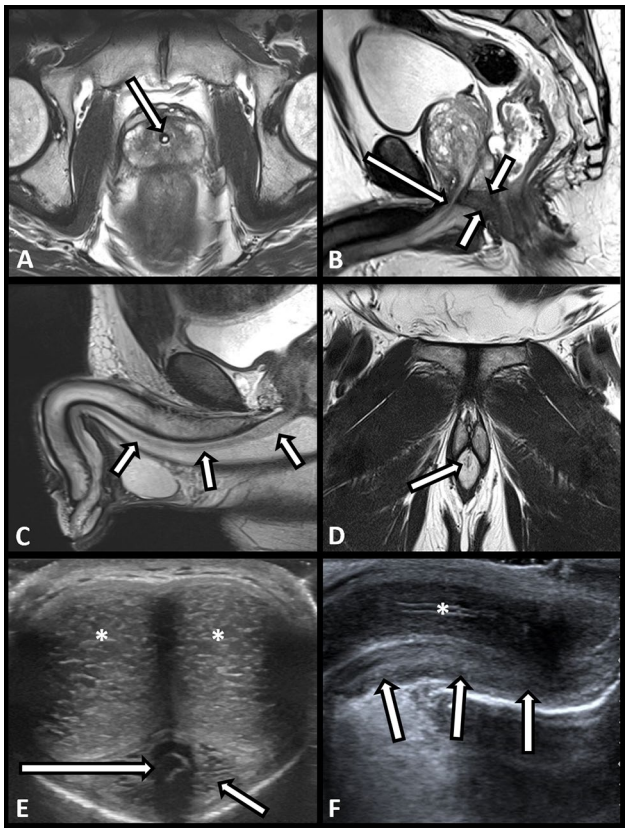

Fig. 5 The urethra (arrow) as depicted on T2-weighted images (T2WI). The prostatic urethra is best seen on axial images (**a**), here demarcated with a Foley catheter. The membranous urethra (long arrow) can be seen as a higher signal structure as it traverses the low signal urogenital diaphragm (short arrows) on sagittal images (**b**). The bulbar and penile urethra can be seen as a linear low signal structure (arrows) within the hyperintense corpus spongiosum on sagittal (**c**) and coronal (**d**) images. With sonography (**e**, **f**), the corpora cavernosa (asterisks) and corpus spongiosum (short arrows) demonstrate bland intermediate intensity echoes. In this case, the urethra (long arrow) within the corpus spongiosum is highlighted by a Foley catheter

Ultrasound

The anterior periurethral tissues of the penis are also well depicted with sonography, although the posterior urethra is typically less well seen. The paired corpora cavernosa and the corpus spongiosum demonstrate a bland pattern of intermediate echogenicity centrally, with the investing tunica albuginea appearing as a thin hyperechoic structure at their periphery (Fig. 5). The urethra is usually not well seen without urethral distention (see discussion below).

Computed tomography

Given the widespread use of CT in the setting of blunt trauma, it is not uncommon to encounter posterior urethral injuries as areas of contrast extravasation on delayed phase images. For the depiction of complex urethral strictures, particularly those accompanied by fistula, CT cystourethrography is a technique which has shown promising results [9–11]. It can be performed as a voiding study after intravenous or direct retrograde contrast injection. Multiplanar 2D and 3D image reconstruction (virtual cystourethroscopy) can facilitate visualization of complex anatomy [9].

Stricture disease

Pathophysiology

Urethral stricture disease refers to a fixed luminal narrowing of the anterior urethra caused by initial urothelial insult followed by scar formation in the surrounding corpus spongiosum (spongiofibrosis) due to collagen and fibroblast proliferation [12–14]. Urinary extravasation into the corpus spongiosum is believed to be an important event in this sequence [15]. The process of insult and scar formation in the urethra can be initiated by several causes, most commonly inflammation (infectious urethritis or lichen sclerosus) and trauma (straddle injury, iatrogenic instrumentation) [5]. Many strictures are also classified as idiopathic [13]. Penile urethral strictures tend to be inflammatory or iatrogenic, whereas bulbous urethral strictures tend to be idiopathic, iatrogenic, or traumatic [15]. Overall, most strictures occur in the bulbous urethra [16].

Fixed narrowing or obliteration of the posterior urethra, commonly called a stenosis rather than a true stricture, is most often initiated by urethral distraction or disruption caused by trauma or surgery [5, 13, 17].

Role of retrograde urethrography

Common presenting symptoms of stricture disease include hesitancy, poor urinary stream, terminal dribbling, and

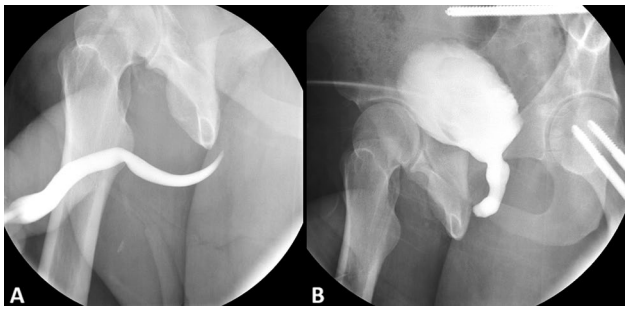

Fig. 6 A 42-year-old male patient sustained blunt pelvic trauma and posterior urethral injury 3 months ago, managed with suprapubic catheterization. Initial RUG (**a**) is unable to reflux contrast into the bladder, making it difficult to distinguish sphincteric spasm from high-grade stricture. Subsequent VCUG (**b**) reveals complete urethral obstruction

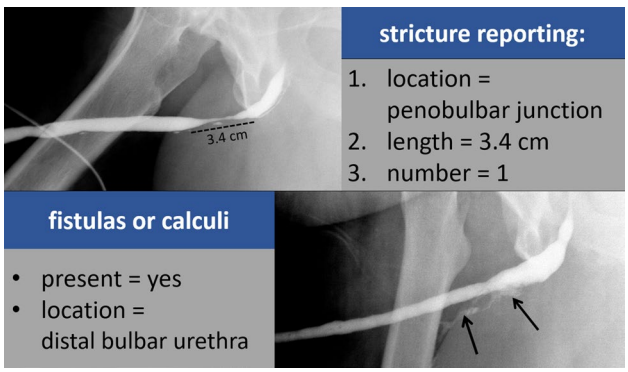

Fig. 7 Examples of stricture reporting. The top image demonstrates an uncomplicated penobulbar stricture. The lower image demonstrates a complicating urethrocutaneous fistula in a different patient

particularly a feeling of incomplete emptying [15]. Given that physical examination is usually not helpful, the most common initial test is RUG [13, 15, 17]. In our experience, a combination of RUG and VCUG provides a more comprehensive evaluation, particularly useful when reflux into the bladder is not possible due to patient intolerance, high-grade stricture, or complete urethral obliteration (Fig. 6). Urethrography can typically provide an accurate estimate of the severity, location, length, and number of strictures (Fig. 7) [5]. Unfortunately, urethrography is not able to assess the degree of spongiofibrosis, the position of the prostate, and abnormalities in the periurethral soft tissues [18]. Additionally, urethrography only provides 2-dimensional images which are dependent on positioning and the degree of penile traction, and results in an average exposure of 1–2 mSv of radiation [19, 20].

Role of ultrasound and MRI

Considering the radiation exposure and limited scope of RUG, the use of ultrasound and MRI has been investigated for a more complete assessment of stricture disease. Sonourethrography (SUG) can be performed with a high-frequency linear array transducer during distention of the urethra with sterile saline or 2% lidocaine hydrochloride jelly, which can be achieved with a balloon tip catheter (balloon inflation at the fossa navicularis) and gentle traction. While SUG provides additional information regarding spongiofibrosis and has been shown to more accurately depict stricture length compared to RUG, it may be less accurate in the diagnosis of posterior urethral pathology [21–24].

Given its excellent soft tissue contrast, it is not surprising that MRI has also been investigated for evaluation of stricture disease. Imaging is typically performed with a phased-array surface coil in a supine patient. Urethral distention can be achieved with retrograde installation of lidocaine jelly or ultrasound gel, or during micturition after the intravenous administration of gadolinium-based contrast media [25, 26]. A soft clamp can be applied to the penile tip to maintain urethral distention during the exam. Strictures are well depicted

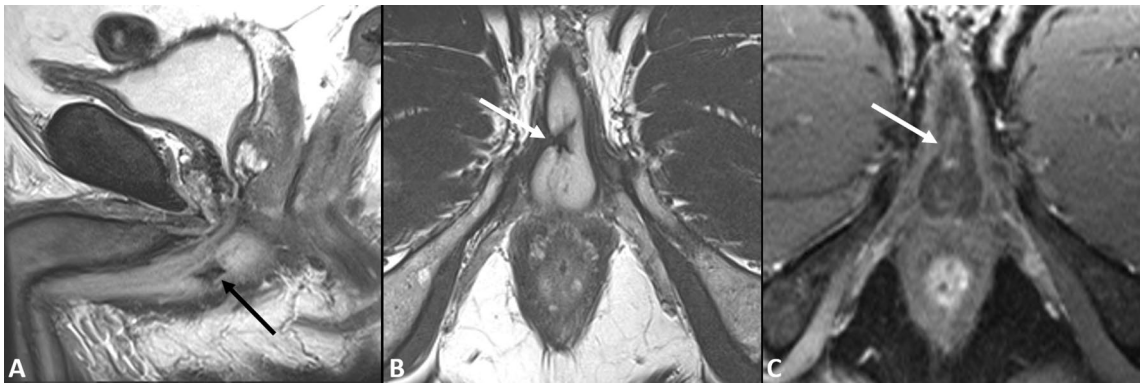

Fig. 8 Typical appearance of spongiofibrosis, with an irregularly shaped T2 hypointense structure (arrows) in the corpus spongiosum adjacent to the urethra on sagittal (**a**) and axial (**b**) T2WI. Delayed enhancement may be noted after contrast (**c**) on T1WI

as focal narrowing of the gel or contrast column, and the adjacent spongiofibrosis can be seen as nodular T2 hypointensity in the hyperintense corpus spongiosum (Fig. 8). MRI has shown accuracy identical to RUG in the diagnosis of stricture, while also providing additional information that would alter treatment, such as the degree of spongiofibrosis, the presence of urethral tumor, and the presence of fistula [25, 27]. MRI-derived stricture measurements have also been shown to better correlate with surgical specimens [18]. An example protocol can be found in Table 1.

Urologic intervention and the role of imaging

The choice of treatment depends on stricture morphology, cause, and any prior surgery [28]. While the traditional approach for symptomatic stricture disease has been dilation or direct visual internal urethrotomy (DVIU), the reported durable success rates are poor [29, 30]. Strictures over 2 cm in length in the penile urethra are particularly prone to recurrence [13]. The UroLume® stent (American Medical Systems, Minnetonka, MN) was used from 1988 to 2011 for recurrent bulbar strictures, but showed high rates of restenosis, stent migration, and other side effects [31]. Those who have failed dilation/DVIU, or those with strictures in the penile urethra or bulbar strictures ≥ 2 cm, tend to benefit from open surgical management—urethroplasty [17]. Urethroplasty is more technically demanding but has higher success rates [32]. Urethroplasty can be categorized into *anastomotic urethroplasty* (stricture excision and primary anastomosis, most commonly performed for short bulbar strictures) and *augmentation urethroplasty* (free graft or flap augments for larger defects) [33]. The more commonly performed repair today is the augmentation urethroplasty, the three types of which are illustrated in Fig. 9.

Conventional urethrography is crucial in the preoperative assessment for possible urethroplasty to describe the location, length, and number of strictures as well as other findings such as fistula. In the postoperative setting, pericatheter RUG has become a standard technique for evaluation of healing without the risk of re-catheterization [34–36]. Catheter removal with VCUG is an alternate approach. Most authors recommend urethrography 2–4 weeks following urethroplasty with a goal of catheter removal at 21–28 days [34, 37, 38]. At our institution, we remove the Foley catheter and perform voiding cystourethrography if no contrast leakage is detected on the initial postoperative pericatheter RUG. A small outpouching is expected at the urethroplasty site and is generally considered normal (Fig. 10). If contrast leakage is present, repeat pericatheter RUG is repeated at 2–3-week intervals until the leak has resolved (Fig. 11). Contrast leakage is relatively common (11.5–64%) and nearly always resolves with continued catheterization, although there is a suggestion that larger leaks (length ≥ 1.0 cm and width ≥ 0.32 cm) may portend higher failure rates after 1 year [34, 36, 37, 39]. Rarely, leaks may not heal and eventually result in urethrocutaneous fistula (Fig. 12). Recurrent stricture is also possible. Risk factors for graft failure include long stricture length, penile location, inflammatory etiology, and previous hypospadias repair (Fig. 13) [32, 40, 41]. The role of urethrography in augmentation urethroplasty is summarized in Fig. 14.

Table 1 Example protocols for MRI of the urethra

Protocol	Sequence	Slice thickness/gap	Orientation	Field of view (cm)	Additional notes
Standard (stricture, trauma, fistula)	T2 FSE	3/1	Axial	24	
	T2 FSE	3/1	Sagittal	24	
	T2 FSE	3/1	Coronal	24	
	T1 FSE	3/1	Axial	24	
	3D T2 FSE	1/0	Sagittal	24	For cases of suspected stricture, performed after urethral distention with sterile lidocaine jelly and application of soft clamp to penile tip
	3D T1 GRE	1/0	Sagittal	20	Pre/post-contrast (30, 60, 90 s); coverage of prostate and penis
Voiding urethrogram (optional for stricture)	3D T1 GRE	1/0	Sagittal	20	Multiphase acquisition without pause (enough phases to cover 60 s). Initiate when patient signals that voiding is imminent. Repeat as necessary
Tumor staging	Fat-suppressed T2 FSE	6/0	Axial	32–40	Cover entire pelvis
	DWI	6/0	Axial	32–40	Cover entire pelvis; multiple *b* values (50, 400, 800 s/mm^2) if scanner allows

The standard protocol is useful for suspected stricture, traumatic injury, or fistula. For fistula evaluation, urethral distention can be achieved with injection of jelly or as a voiding study. Larger FOV T2WI and DWI are added in cases of tumor staging to assess regional lymph nodes

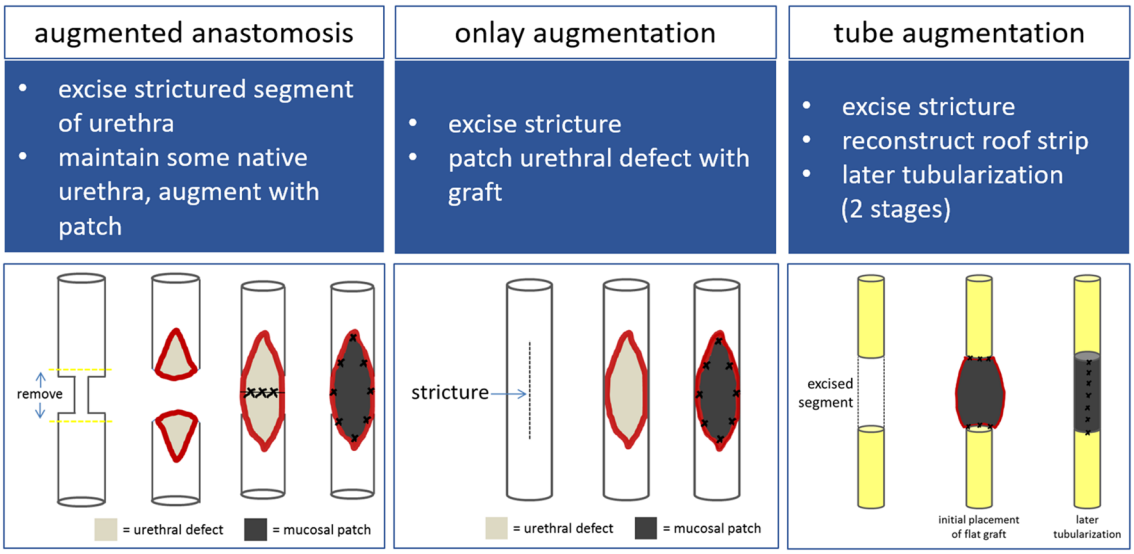

Fig. 9 Illustration of the three most commonly performed augmentation urethroplasty techniques

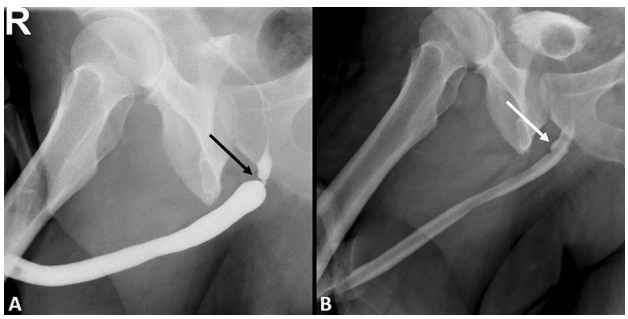

Fig. 10 A 34-year-old male with a short high-grade bulbar stricture (black arrow **a**) undergoes augmentation urethroplasty. 3 weeks after surgery, a pericatheter RUG (**b**) shows a tiny outpouching (white arrow) at the repair site, but no extravasation. This is considered a normal finding

Traumatic urethral injury

Blunt injury

Blunt urethral trauma is usually classified as either anterior or posterior in location. While anterior injuries are usually due to straddle-type injuries of the bulbar urethra, posterior injuries are usually due to a crushing force to the pelvis and are found in 4–14% of patients with pelvic fractures [42]. Anterior injuries may also be accompanied by penile fracture (disruption of the tunica albuginea of the corpus cavernosum) [43]. Bladder lacerations are seen in 20% of patients with posterior injuries [44].

After initial attention to management of life-threatening injuries in those presenting with pelvic trauma,

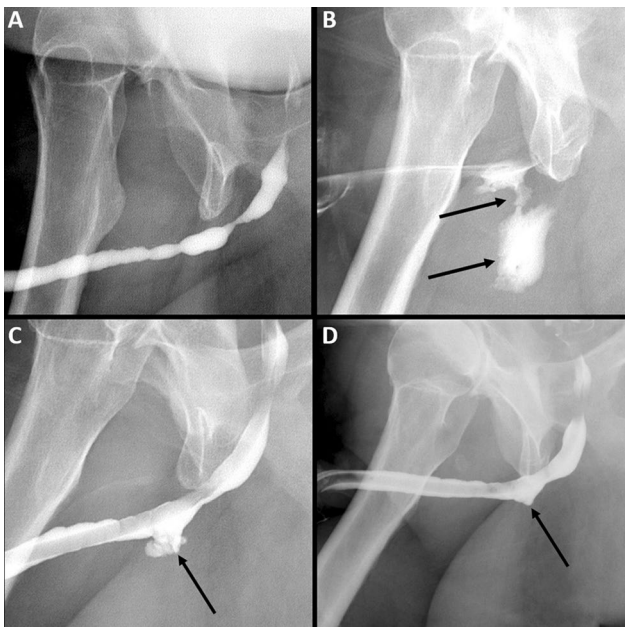

Fig. 11 A patient with multifocal bulbar and penile strictures (**a**) undergoes a complex augmentation urethroplasty repair. The initial pericatheter RUG 4 weeks later (**b**) reveals gross contrast extravasation (arrows). After another 3 weeks, the contrast is contained (arrow, **c**), with only a small outpouching visible after a further 3 weeks (arrow, **d**) of management with Foley catheter drainage

RUG should be considered the initial study of choice in a hemodynamically stable patient with blood at the meatus or other risk factors such as an inability to void, hematoma of the penis or perineum, or "high-riding" prostate noted at rectal examination, prior to catheter insertion [3].

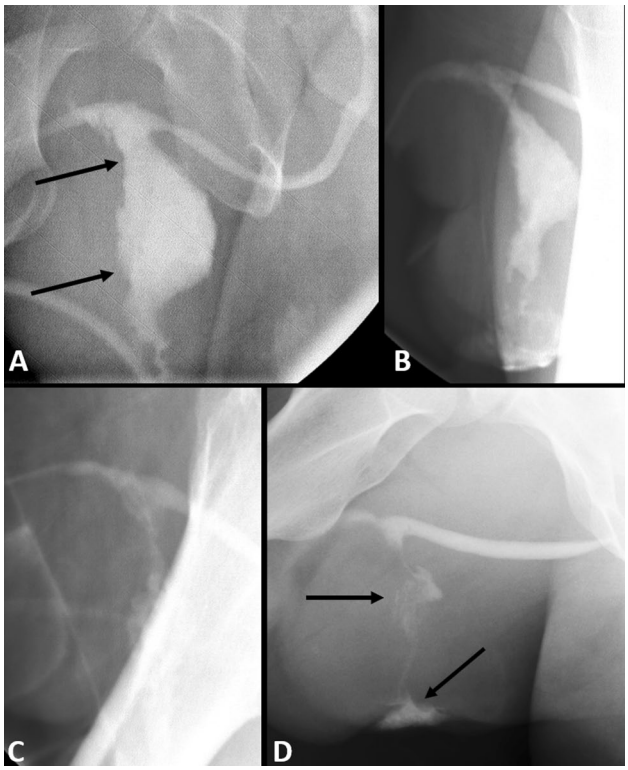

Fig. 12 Initial RUG 3 weeks after augmentation urethroplasty with a large amount of contrast extravasation (arrows **a**). Subsequent examinations 3 (**b**) and 6 (**c**) weeks later demonstrate continued extravasation. At 11 weeks after surgery (**d**), a fistula (arrows) to the perineum has developed. Penile stricture location is a risk factor for failed urethroplasty

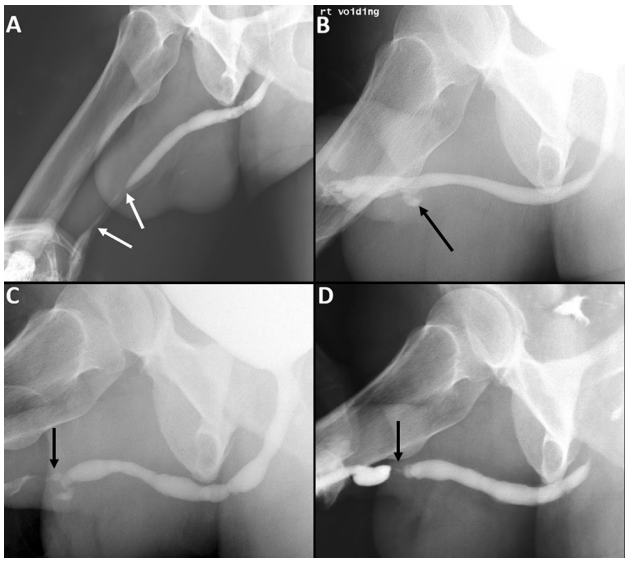

Fig. 13 Long penile stricture in a patient with prior hypospadias repair (arrows **a**). Initial VCUG following urethroplasty demonstrates improved stricture with small outpouching (arrow **b**), expected findings. Follow-up RUGs at 3-week intervals (**c**, **d**) demonstrate progressive stricture (arrows) at the repair site. History of hypospadias, penile location, and long stricture length are all risk factors for graft failure

Posterior urethral and bladder injuries also commonly result in edema and hematoma formation in the prostate and bladder base on trauma CT scans as well. A suprapubic catheter is placed if a urethral injury is noted on the initial RUG and can facilitate later VCUG. Delayed repair is the most common approach. MRI has also been shown to be useful in surgical planning, particularly for detection of co-existing penile fracture, identification of urethral distraction defect, and evaluation of the degree of prostatic displacement [45–47]. Combined RUG/VCUG can also be useful for delineation of urethral transection and high-grade stricture (Fig. 6).

Accurate classification of urethral injuries is crucial for treatment planning. The Goldman system, a modification of initial work by Colapinto and McCallum, describes five types of injury based on its anatomic location [42, 44]. The system advocated by the American Association for the Surgery of Trauma (AAST) categorizes injuries according to the treatment required, rather than precise location, with a greater emphasis on the degree of urethral disruption and separation (Table 2) [48]. The provided example cases (Fig. 15) illustrate the Goldman system. Complete disruption of the membranous urethra can occur in Goldman II and III patterns, resulting in a superiorly dislocated bladder with the "pie in the sky" appearance after intravenous contrast (Fig. 16). Stricture is almost certain following severe injury at any site. Urinary incontinence can occur after Goldman III injuries of the external sphincter; erectile dysfunction is a less common delayed complication after anterior or posterior urethral injury [5].

Penile fracture and penetrating injury

Two additional injury patterns not included in either classification system are penile fracture and penetrating urethral injury. Penetrating penile injury requires RUG because up to 50% of patients will have urethral injury (Fig. 17), and most require surgical exploration [5]. As urethral injury occurs in 38% of penile fracture cases (Fig. 18), RUG is generally indicated if fracture is clinically suspected [5]. Fracture most commonly involves disruption of the tunica albuginea of one, and rarely both, of the corpora cavernosa. The corpus spongiosum can also be injured [49]. MRI is the examination of choice when further evaluation of cavernosal injury is required, given the excellent anatomic depiction [45, 50]. Disruption of the tunica albuginea is well depicted on T2-weighted imaging, usually accompanied by adjacent edema and hematoma formation (Fig. 19). Ultrasound has also shown promise in the diagnosis of penile fracture (Fig. 19) [51].

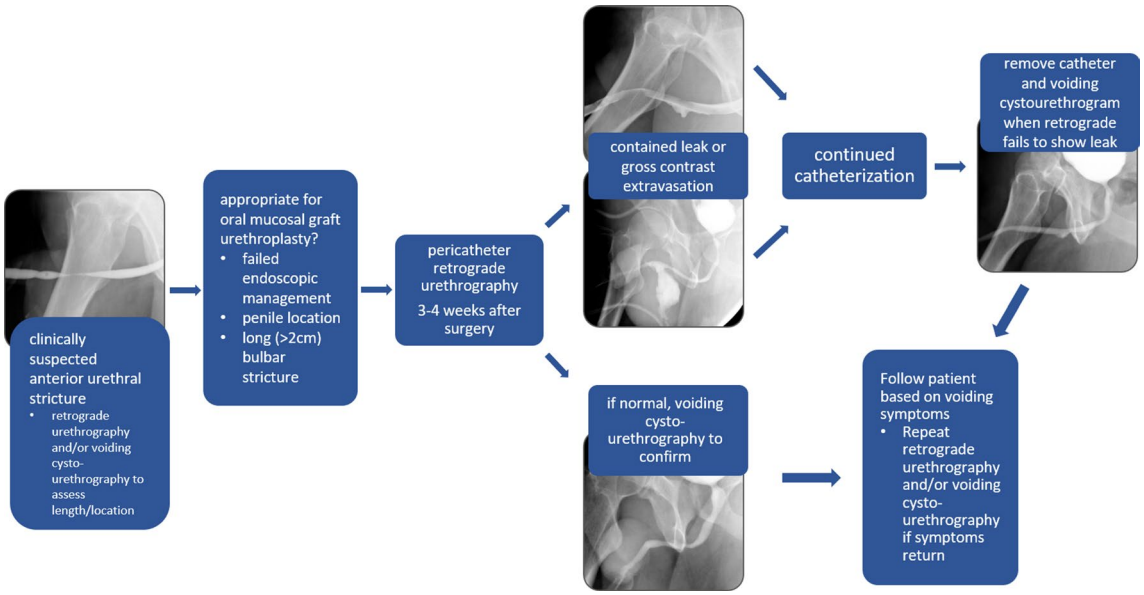

Fig. 14 Role of urethrography in augmentation urethroplasty

Table 2 American Association for the Surgery of Trauma (AAST) classification of blunt urethral trauma. Adapted from Moore et al. [48]

Injury type	Injury description	Urethrographic appearance	Treatment
1	Contusion	Normal	None
2	Stretch injury	Elongation of the urethra without extravasation	Conservative—suprapubic/urethral catheter
3	Partial disruption	Extravasation of contrast media from the urethra with bladder opacification	Conservative—suprapubic/urethral catheter
4	Complete disruption	Extravasation of contrast media from the urethra without bladder opacification. Urethral separation < 2 cm	Endoscopic realignment or delayed graft urethroplasty
5	Complete disruption	Extravasation of contrast media from the urethra without bladder opacification. Urethral separation < 2 cm	Endoscopic realignment or delayed graft urethroplasty

Implant complications

The use of artificial urinary sphincters (AUS) for the treatment of urinary incontinence has become relatively common in the past 2 decades [52, 53]. While AUS has been shown to be effective, a revision rate of 31% means that complications such as erosion, urethral atrophy, and mechanical failure are not uncommon [54]. Most cases of erosion are diagnosed on cystoscopy, although RUG and VCUG can be useful in postoperative evaluation after implant removal (Fig. 20). The epithelializing urethral stent (UroLume®) was also widely used from 1988 until 2011 for bulbous urethral strictures, with promising early results [31]. Unfortunately, one in six men ultimately required stent removal due to complications such as restenosis, stent migration, and urinary infection [31, 55]. RUG and VCUG can readily demonstrate recurrent in-stent stricture (Fig. 20).

Fistula

Urethral fistulas can be complex, and their precise delineation is often quite difficult for both the clinician and the radiologist. Urethral fistulas may communicate with any number of structures, including the perineum, rectum, and scrotum [43]. Infection and/or inflammation are common causes, although fistulas can also occur after pelvic surgery and radiation. Active fistulas in the anterior urethra are more commonly seen with RUG than those in the posterior urethra (Fig. 21) [1]. At our institution, we have found MRI to be a useful technique for fistula mapping and depiction of causative pathology such as abscess and tumor. Actively draining fistula tracts are usually T2 hyperintense and demonstrate post-contrast enhancement, particularly in the delayed phase (Fig. 22).

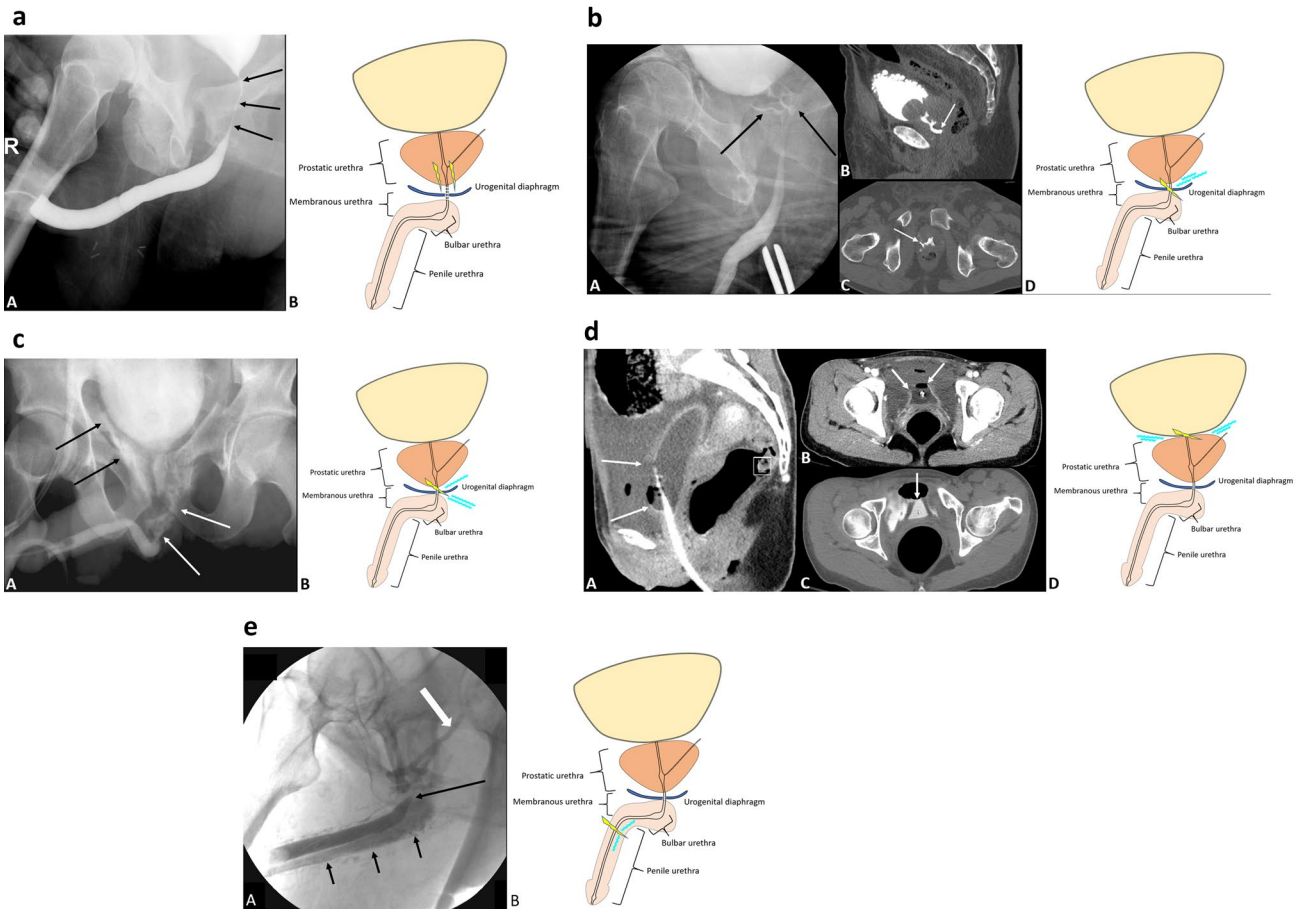

Fig. 15 **a** Goldman I: rupture of the puboprostatic ligaments results in stretching of the intact prostatic urethra. At RUG (**A**), the posterior urethra appears narrow and elongated (arrows). No contrast extravasation is expected. **B** Accompanying anatomic depiction with site of injury (jagged tear). **b** Goldman II: the membranous urethra is injured above an intact urogenital diaphragm. At RUG (**A**), contrast is expected to extravasate above the diaphragm in the extraperitoneal space (arrows) but *not* in the perineum. At delayed phase CT (**B**, **C**), extraluminal contrast (arrows) is visible at the prostatic apex above the diaphragm. **D** Anatomic depiction demonstrating site of injury (jagged tear) and resultant pattern of extravasation (rivulets). **c** Goldman III: in this the most common injury pattern, both the membranous and bulbous urethra are injured along with the urogenital diaphragm. At RUG (**A**), contrast extravasation occurs *below* the diaphragm (white arrows) and can also be seen in the extraperitoneal space superiorly (black arrows). (**B**) Anatomic depiction demonstrating site of injury (jagged tear) and resultant pattern of extravasation (rivulets). **d** Goldman IV/IVa: in the IV pattern, the bladder neck is injured, often including the internal sphincter. In the IVa pattern, the bladder base is injured but the bladder neck is *not* involved. These are typically indistinguishable from one another with imaging. Portal venous phase CT images (**A**, **B**) reveal a disruption in the bladder base (arrows) with extraperitoneal fluid. Delayed phase scan reveals extraperitoneal contrast extravasation through the defect (arrow). **D** Anatomic depiction demonstrating site of injury (jagged tear) and possible extravasation patterns (rivulets). **e** Goldman V: isolated anterior urethra straddle injury, in which the bulbous urethra and corpus spongiosum are compressed between an object and the inferior aspect of the pubic bones. At RUG, the extravasation pattern varies depending on the extent of urethral and fascial (Buck, Colle) injury. In this example (**A**), there is immediate venous intravasation at the site of bulbous urethral discontinuity (long black arrow), with opacification of corpus spongiosum (short black arrows) and draining veins (white arrow). Venous intravasation is common in this injury pattern. **B** Anatomic depiction demonstrating anterior urethra injury (jagged tear) and contrast extravasation (rivulets) into the corpus spongiosum

Tumor

Urethral malignancy is rare, and more common in men than women [56]. In men, most cases (78%) are urothelial carcinoma, with squamous cell carcinoma (12%) and adenocarcinoma (5%) occurring less commonly [57]. Approximately 60% occur in the bulbomembranous region, 30% in the penile urethra, and 10% in the prostatic urethra [43]. An understanding of the pathology continues to evolve, but recent data suggest that primary urethral carcinomas may be a unique biologically aggressive hybrid tumor, possibly associated with human papilloma virus [58]. Symptoms are quite variable. As obstructive symptoms are not uncommon, RUG/VCUG may often be the initial examination. It is therefore important for

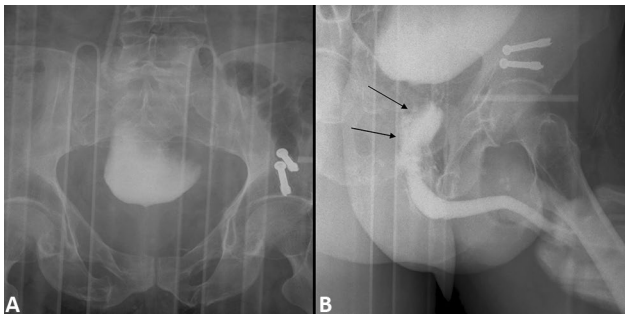

Fig. 16 This patient with multiple pelvic fractures experienced complete disruption of the membranous urethra. On initial intravenous urogram (**a**), the bladder is elevated due to loss of attachment and accompanying hematoma. Contrast extravasation (arrows) at subsequent RUG (**b**) without reflux into the bladder

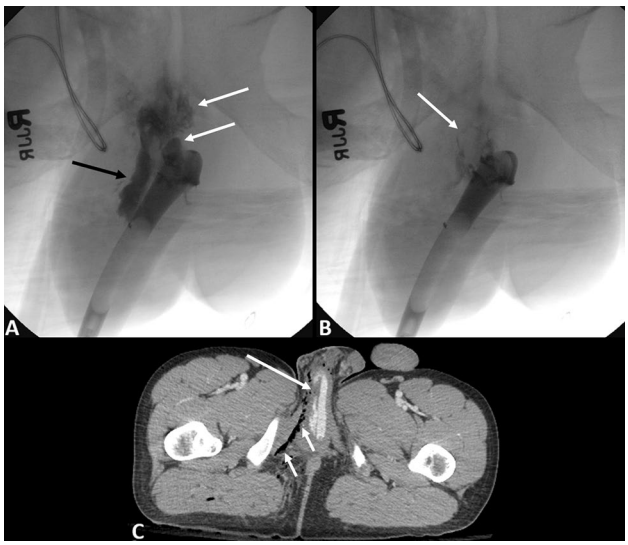

Fig. 17 A 23-year-old male presents after a gunshot wound to the pelvis. Early image from RUG (**a**) demonstrates contrast extravasation (white arrows) from the bulbous urethra, as well as opacification of corpus cavernosum (black arrow). Later image shows draining veins (arrow **b**). On the portal venous phase CT scan, the injured right corpus cavernosum (long arrow) has diminished enhancement. Soft tissue gas (short arrows) demarcates the bullet trajectory

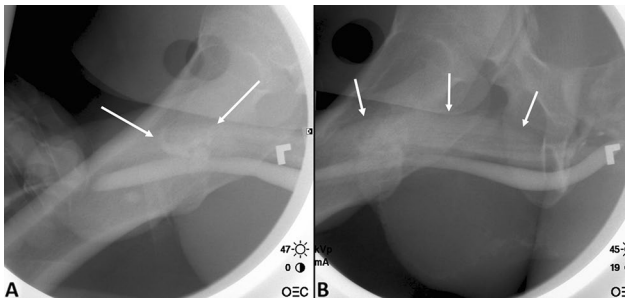

Fig. 18 RUG in a patient presenting with clinically suspected penile fracture demonstrates initial contrast extravasation from the dorsal penile urethra (arrows, **a**), followed by opacification of the corpus cavernosum (arrows, **b**) indicating injury to the tunica albuginea

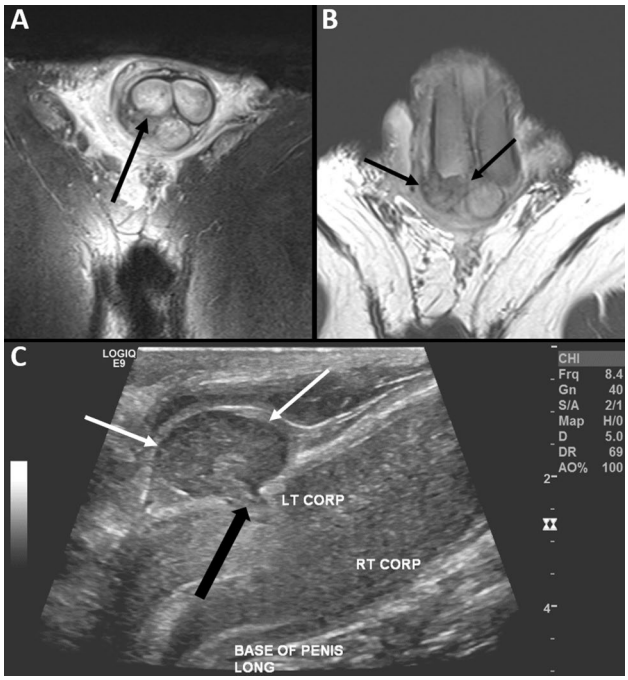

Fig. 19 In one patient with clinically suspected penile fracture, coronal T2-weighted MRI reveals focal disruption of the right posterior tunica albuginea (arrow, **a**) with surrounding high signal edema. The adjacent hematoma is well seen on axial T1-weighted image (arrows, **b**). In a second patient, high-resolution sonography (**c**) through the penile base depicts the focal defect in the tunica albuginea (black arrow), with adjacent hematoma formation (white arrows)

the radiologist to carefully assess sites of stricture for mass-like filling defects, mucosal irregularities, and any degree of luminal expansion (Fig. 23). High-grade stricture, arresting the contrast column, should also be carefully approached (Fig. 24). Once a diagnosis is made, typically with endoscopic biopsy, staging is indicated for treatment planning. MRI has emerged as the method of choice for evaluating local tumor extent, while also identifying lymphatic disease using larger fields of view [1, 43, 59]. In addition to size and location, the degree of periurethral invasion is perhaps most important for treatment planning. In particular, the corpus spongiosum, prostate gland, prostate capsule, corpus cavernosum, and bladder neck should be scrutinized for involvement (Table 3). Tumors are typically hypointense to adjacent corpus spongiosum on T2WI with modest enhancement on T1WI following contrast administration. T2 signal can be increased with associated inflammation. Fistulas are not uncommon and are well depicted with MRI (Fig. 23). In a series of 106 primary urethral carcinomas, Zhang et al. found the inguinal stations

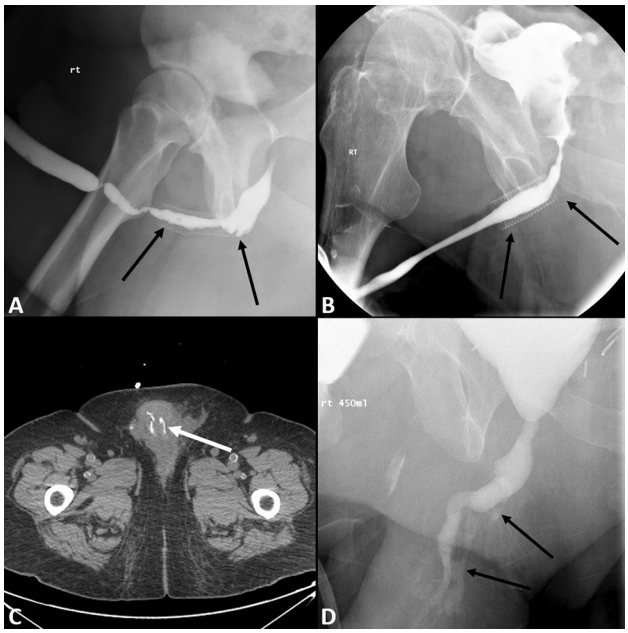

Fig. 20 **a** A 47-year-old male presented with a complex history of strictures, currently managed with a suprapubic catheter. UroLume® stent (arrows) in the bulbar and penile urethra. Note the multifocal strictures, including inside the stent. This patient subsequently underwent successful stent explantation and augmented urethroplasty. **b** A 73-year-old male underwent UroLume® stent placement following a failed trans-urethral resection of the prostate for BPH. Although the stent (arrows) remains patent, he developed urinary incontinence eventually requiring urinary diversion. **c** A 78-year-old male underwent artificial urethral sphincter placement for incontinence. Arrow denotes the cuff surrounding the bulbous urethra. After development of a urethrocutaneous fistula with purulent drainage, the device was removed. Follow-up VCUG (**d**) demonstrates bulbous urethral irregularity and contrast extravasation from the site (arrows)

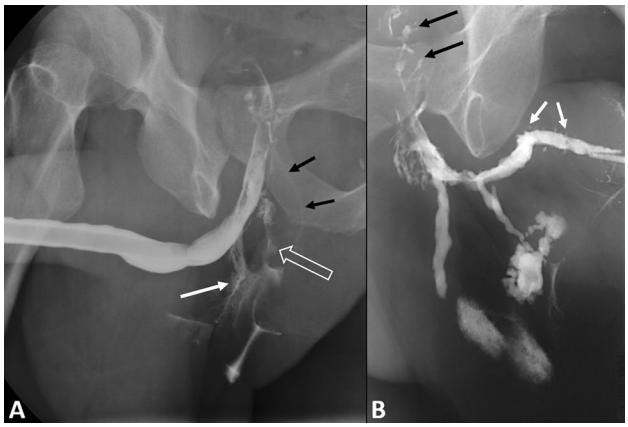

Fig. 21 Patient with perianal fistulizing Crohn disease (**a**) and faintly visible seton (short black arrows). One urethral fistula (hollow arrow) extends to the seton, while a second tract opens to the perineum (solid white arrow). In another patient (**b**) with a history of gonorrhea, at least two urethrocutaneous fistulas are present, as well as areas of outward contrast excavation at sites of paraurethral abscess, resulting in the classic "watering can perineum." Opacification of prostatic ducts (black arrows) and periurethral Littre glands (white arrows) is often, but not always, associated with inflammatory disease

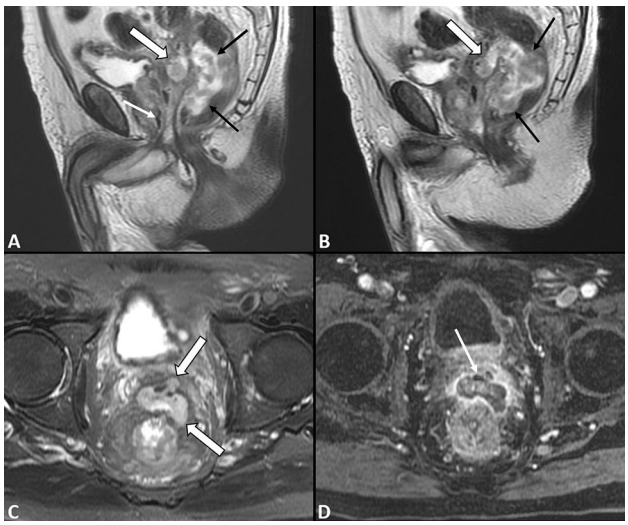

Fig. 22 A 90-year-old male with known rectal mass and development of pneumaturia. Hyperintense fistula tract (thick white arrows) extends anteriorly from the mass (black arrows), as seen on sagittal (**a**, **b**) and axial (**c**) T2WI. Peripheral enhancement along the tract is noted after contrast on T1WI (**d**). Note the signal void (thin white arrows) in the prostatic urethra (**a**) and fistula tract (**d**) due to gas from the rectum

to be the most commonly involved by regional nodal metastases, and the lung and liver to be the most common sites of hematogenous metastasis [58].

Conclusions

As we have demonstrated with numerous case examples, retrograde urethrography and voiding cystourethrography remain integral components in the diagnosis of most major urethral pathology in the male patient, including stricture disease, traumatic injury, fistulas, and neoplasia. To provide the most clinically useful information, the radiologist must have a thorough understanding of urethral anatomy, disease pathophysiology, and how both can be depicted with a technically superb examination. Case examples of trauma and neoplasia have also highlighted the value of MRI in urethral evaluation when disease extends to involve the periurethral soft tissues. We have also shown the importance of imaging in the planning and postoperative evaluation for those patients undergoing augmented urethroplasty for stricture disease.

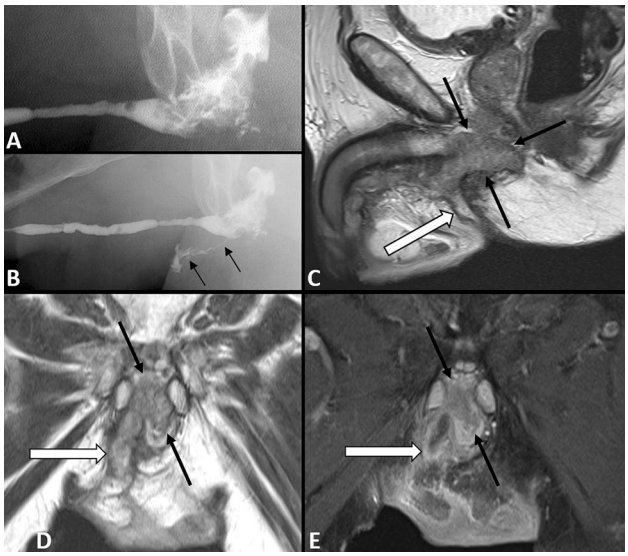

Fig. 23 RUG (**a**, **b**) is performed to assess for hematuria and irregular urinary stream. In addition to multifocal penile strictures, the bulbous urethra is expanded with mass-like filling defects, suggesting neoplasm. Later phase image (**b**) also demonstrates a urethrocutaneous fistula (black arrows). Sagittal (**c**) and coronal (**d**) T2WI demonstrate a slightly hypointense mass (black arrows) replacing the bulbous urethra, along with the fistula (thick white arrows). Expected modest tumoral enhancement on coronal T1WI (black arrows, **e**). Surgical pathology revealed squamous cell carcinoma

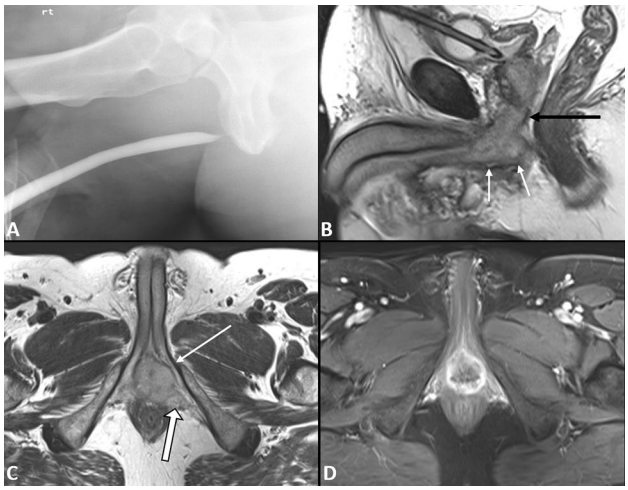

Fig. 24 Urinary symptoms led to RUG (**a**) for suspected urethral stricture, currently managed with suprapubic catheter. A high-grade stricture of the bulbous urethra was indeed present. At time of urethroplasty, unexpected tumor was encountered. Subsequent MRI was performed for staging. Sagittal (**b**) and axial (**c**) T2WI demonstrates an intermediate signal mass in the bulbous urethra, invading the prostatic apex (black arrow), bulbospongiosus (short white arrows), and transverse perineal (thick white arrow) muscles, and threatening the left crus of corpus cavernosum (long thin white arrow). Enhancement is noted after contrast on T1WI (**d**). Surgical pathology revealed invasive squamous cell carcinoma

Table 3 TNM staging of primary urethral carcinoma. Adapted from Hartman and Kawashima [56]

Classification	Definition
T	Primary tumor
T1	Tumor invades subepithelial connective tissue
T2	Tumor invades corpus spongiosum, prostate, or periurethral muscle
T3	Tumor invades corpus cavernosum, beyond prostate capsule, or bladder neck
T4	Tumor invades adjacent organs
N	Regional lymph nodes
N0	No regional lymph node metastasis
N1	Metastasis in a single lymph node 2 cm or less in greatest dimension
N2	Metastasis in a single lymph node > 2 cm in greatest dimension, or in multiple lymph nodes
M	Distant metastasis
M0	No distant metastasis
M1	Distant metastasis

References

1. Kim B, Kawashima A, LeRoy AJ (2007) Imaging of the male urethra. Semin Ultrasound CT MR 28(4):258-273
2. Sandler CM, Corriere JN (1989) Urethrography in the diagnosis of acute urethral injuries. Urol Clin North Am 16(2):283-289
3. Ingram MD, Watson SG, Skippage PL, Patel U (2008) Urethral injuries after pelvic trauma: evaluation with urethrography. Radiographics 28(6):1631-1643
4. Berná-Mestre JD, Berná-Serna JD, Aparicio-Mesón M, Canteras-Jordana M (2009) Urethrography in men: conventional technique versus clamp method. Radiology 252(1):240-246
5. Kawashima A, Sandler CM, Wasserman NF, LeRoy AJ, King BF, Goldman SM (2004) Imaging of urethral disease: a pictorial review. Radiographics 24 Suppl1:S195-216
6. Kirkham A (2012) MRI of the penis. Br J Radiol 85 Spec No 1:S86-93
7. Kochhar R, Taylor B, Sangar V (2010) Imaging in primary penile cancer: current status and future directions. Eur Radiol 20(1):36-47
8. Scardino E, Villa G, Bonomo G, Matei DV, Verweij F, Rocco B, Varela R, de Cobelli O (2004) Magnetic resonance imaging combined with artificial erection for local staging of penile cancer. Urology 63(6):1158-1162
9. Feng C, Shen YL, Xu YM, Fu Q, Sa YL, Xie H, Lv XG (2014) CT virtual cystourethroscopy for complex urethral strictures: an investigative, descriptive study. Int Urol Nephrol 46(5):857-863
10. Lv XG, Peng XF, Feng C, Xu YM, Shen YL (2016) The application of CT voiding urethrography in the evaluation of urethral stricture associated with fistula: a preliminary report. Int Urol Nephrol 48(8):1267-1273
11. Zhang XM, Hu WL, He HX, Lv J, Nie HB, Yao HQ, Yang H, Song B, Peng GM, Liu HL (2011) Diagnosis of male posterior urethral stricture: comparison of 64-MDCT urethrography vs. standard urethrography. Abdom Imaging 36(6):771-775
12. Gallentine ML, Morey AF (2002) Imaging of the male urethra for stricture disease. Urol Clin North Am 29(2):361-372
13. Mangera A, Osman N, Chapple C (2016) Evaluation and management of anterior urethral stricture disease. F1000Res. https://doi.org/10.12688/f1000research.7121.1

14. Shahsavari R, Bagheri SM, Iraji H (2017) Comparison of diagnostic value of sonourethrography with retrograde urethrography in diagnosis of anterior urethral stricture. Open Access Maced J Med Sci 5(3):335-339
15. Mundy AR, Andrich DE (2011) Urethral strictures. BJU Int 107(1):6-26
16. Stein DM, Thum DJ, Barbagli G, Kulkarni S, Sansalone S, Pardeshi A, Gonzalez CM (2013) A geographic analysis of male urethral stricture aetiology and location. BJU Int 112(6):830-834
17. Wessells H, Angermeier KW, Elliot SP, et al. (2016) Male Urethral Stricture. American Urological Association Clinical Guidelines. https://www.auanet.org/guidelines/urethral-stricture-guideline. Accessed 27 March 2019
18. Sung DJ, Kim YH, Cho SB, Oh YW, Lee NJ, Kim JH, Chung KB, Moon du G, Kim JJ (2006) Obliterative urethral stricture: MR urethrography versus conventional retrograde urethrography with voiding cystourethrography. Radiology 240(3):842-848
19. Theisen KM, Kadow BT, Rusilko PJ (2016) Three-dimensional imaging of urethral stricture disease and urethral pathology for operative planning. Curr Urol Rep. https://doi.org/10.1007/s11934-016-0616-0
20. Hart D, Wall BF (2004) UK population dose from medical X-ray examinations. Eur J Radiol 50(3):285-291
21. Gupta S, Majumdar B, Tiwari A, Gupta RK, Kumar A, Gujral RB (1993) Sonourethrography in the evaluation of anterior urethral strictures: correlation with radiographic urethrography. J Clin Ultrasound 21(4):231-239
22. Buckley JC, Wu AK, McAninch JW (2012) Impact of urethral ultrasonography on decision-making in anterior urethroplasty. BJU Int 109(3):438-442
23. Ravikumar BR, Tejus C, Madappa KM, Prashant D, Dhayanand GS (2015) A comparative study of ascending urethrogram and sono-urethrogram in the evaluation of stricture urethra. Int Braz J Urol 41(2):388-392
24. Bryk DJ, Khurana K, Yamaguchi Y, Kozirovsky M, Telegrafi S, Zhao LC (2016) Outpatient ultrasound urethrogram for assessment of anterior urethral stricture: early experience. Urology 93:203-207
25. Osman Y, El-Ghar MA, Mansour O, Refaie H, El-Diasty T (2006) Magnetic resonance urethrography in comparison to retrograde urethrography in diagnosis of male urethral strictures: is it clinically relevant? Eur Urol 50(3):587-593
26. Yekeler E, Suleyman E, Tunaci A, Tunaci M, Balci NC, Onem K, Tunc M, Acunas G (2004) Contrast-enhanced 3D MR voiding urethrography: preliminary results. Magn Reson Imaging 22(9):1193-1199
27. Hanna S, Abdel Rahman S, Altamimi B, Shoman AM (2015) Role of MR urethrography in assessment of urethral lesions. Epypt J Radiol Nuclear Med 46:499-505
28. Chapple C, Andrich D, Atala A, Barbagli G, Cavalcanti A, Kulkarni S, Mangera A, Nakajima Y (2014) SIU/ICUD consultation on urethral strictures: the management of anterior urethral stricture disease using substitution urethroplasty. Urology 83(3 Suppl):S31-47
29. Pansadoro V, Emiliozzi P (1996) Internal urethrotomy in the management of anterior urethral strictures: long-term followup. J Urol 156(1):73-75
30. van Leeuwen MA, Brandenburg JJ, Kok ET, Vijverberg PL, Bosch JL (2011) Management of adult anterior urethral stricture disease: nationwide survey among urologists in the Netherlands. Eur Urol 60(1):159-166
31. Angulo JC, Kulkarni S, Pankaj J, Nikolavsky D, Suarez P, Belinky J, Virasoro R, DeLong J, Martins FE, Lumen N, Giudice C, Suárez OA, Menéndez N, Capiel L, López-Alvarado D, Ramirez EA, Venkatesan K, Husainat MM, Esquinas C, Arance I, Gómez R, Santucci R (2018) Urethroplasty after urethral Urolume stent: an international multicenter experience. Urology 118:213-219
32. Spilotros M, Sihra N, Malde S, Pakzad MH, Hamid R, Ockrim JL, Greenwell TJ (2017) Buccal mucosal graft urethroplasty in men - risk factors for recurrence and complications: a third referral centre experience in anterior urethroplasty using buccal mucosal graft. Transl Androl Urol 6(3):510-516
33. Horiguchi A (2017) Substitution urethroplasty using oral mucosa graft for male anterior urethral stricture disease: Current topics and reviews. Int J Urol 24(7):493-503
34. Solanki S, Hussain S, Sharma DB, Solanki FS, Sharma D (2014) Evaluation of healing at urethral anastomotic site by pericatheter retrograde urethrogram in patients with urethral stricture. Urol Ann 6(4):325-327
35. Balogun BO, Ikuerowo SO, Akintomide TE, Esho JO (2009) Retrograde pericatheter urethrogram for the post-operative evaluation of the urethra. Afr J Med Med Sci 38(2):131-134
36. Sussman RD, Hill FC, Koch GE, Patel V, Venkatesan K (2017) Novel pericatheter retrograde urethrogram technique is a viable method for postoperative urethroplasty imaging. Int Urol Nephrol 49(12):2157-2165
37. Grossgold ET, Eswara JR, Siegel CL, Vetter J, Brandes SB (2017) Routine Urethrography After Buccal Graft Bulbar Urethroplasty: The impact of initial urethral leak on surgical success. Urology 104:215-219
38. Santucci RA, Mario LA, McAninch JW (2002) Anastomotic urethroplasty for bulbar urethral stricture: analysis of 168 patients. J Urol 167(4):1715-1719
39. Bansal A, Singh V, Sinha R (2017) Retrograde pericatheter urethrography technique and its clinical use after urethroplasty: a single center experience. African J. Urol 23(1):68-71
40. Wang K, Miao X, Wang L, Li H (2009) Dorsal onlay versus ventral onlay urethroplasty for anterior urethral stricture: a meta-analysis. Urol Int 83(3):342-348
41. Chauhan S, Yadav SS, Tomar V (2016) Outcome of buccal mucosa and lingual mucosa graft urethroplasty in the management of urethral strictures: a comparative study. Urol Ann 8(1):36-41
42. Colapinto V, McCallum RW (1977) Injury to the male posterior urethra in fractured pelvis: a new classification. J Urol 118(4):575-580
43. Ryu J, Kim B (2001) MR imaging of the male and female urethra. Radiographics 21(5):1169-1185
44. Goldman SM, Sandler CM, Corriere JN, McGuire EJ (1997) Blunt urethral trauma: a unified, anatomical mechanical classification. J Urol 157(1):85-89
45. Saglam E, Tarhan F, Hamarat MB, Can U, Coskun A, Camur E, Sarica K (2017) Efficacy of magnetic resonance imaging for diagnosis of penile fracture: a controlled study. Investig Clin Urol 58(4):255-260
46. da Silva Gaspar SR, Ferreira ND, Oliveira T, Oliveira P, Dias JS, Lopes TM (2017) Magnetic resonance imaging and pelvic fracture urethral injuries. Urology 110:9-15
47. Pandian RM, John NT, Eapen A, Antonisamy B, Devasia A, Kekre N (2017) Does MRI help in the pre - operative evaluation of pelvic fracture urethral distraction defect? - a pilot study. Int Braz J Urol 43(1):127-133
48. Moore EE, Cogbill TH, Malangoni MA, Jurkovich GJ, Shackford SR, Champion HR, McAninch JW (1995) Organ injury scaling. Surg Clin North Am 75(2):293-303
49. Mirzazadeh M, Fallahkarkan M, Hosseini J (2017) Penile fracture epidemiology, diagnosis and management in Iran: a narrative review. Transl Androl Urol 6(2):158-166
50. Guler I, Ödev K, Kalkan H, Simsek C, Keskin S, Kilinç M (2015) The value of magnetic resonance imaging in the diagnosis of penile fracture. Int Braz J Urol 41(2):325-328

51. Zare Mehrjardi M, Darabi M, Bagheri SM, Kamali K, Bijan B (2017) The role ofultrasound (US) and magnetic resonance imaging (MRI) in penile fracture mapping for modified surgical repair. Int Urol Nephrol 49(6):937-945
52. Abello A, Das AK (2019) Long-term (> 5 years) outcomes of patients implanted with artificial urinary sphincter: a single-center experience. Urol Ann 11(1):15-19
53. Loh-Doyle JC, Ashrafi A, Nazemi A, Ghodoussipour S, Thompson E, Wayne K, Boyd SD (2019) Dual prosthetic implantation after radical cystoprostatectomy and neobladder: outcomes of the inflatable penile prosthesis and artificial urinary sphincter in bladder cancer survivors. Urology. https://doi.org/10.1016/j.urology.2019.01.010
54. Tutolo M, Cornu JN, Bauer RM, Ahyai S, Bozzini G, Heesakkers J, Drake MJ, Tikkinen KAO, Launonen E, Larré S, Thiruchelvam N, Lee R, Li P, Favro M, Zaffuto E, Bachmann A, Martinez-Salamanca JI, Pichon T, De Nunzio C, Ammirati E, Haab F, Van Der Aa F (2019) Efficacy and safety of artificial urinary sphincter (AUS): results of a large multi-institutional cohort of patients with mid-term follow-up. Neurourol Urodyn 38(2):710-718
55. Armitage JN, Cathcart PJ, Rashidian A, De Nigris E, Emberton M, van der Meulen JH (2007) Epithelializing stent for benign prostatic hyperplasia: a systematic review of the literature. J Urol 177(5):1619-1624
56. Hartman R, Kawashima A (2017) Lower tract neoplasm: Update of imaging evaluation. Eur J Radiol 97:119-130
57. Rabbani F (2011) Prognostic factors in male urethral cancer. Cancer 117(11):2426-2434
58. Zhang M, Adeniran AJ, Vikram R, Tamboli P, Pettaway C, Bondaruk J, Liu J, Baggerly K, Czerniak B (2018) Carcinoma of the urethra. Hum Pathol 72:35-44
59. Stewart SB, Leder RA, Inman BA (2010) Imaging tumors of the penis and urethra. Urol Clin North Am 37(3):353-367